# Activation-Driven Programmed Cell Death and T Cell Receptor ζη Expression

MLADEN MERĆEP, ALLAN M. WEISSMAN,* STUART J. FRANK, RICHARD D. KLAUSNER, JONATHAN D. ASHWELL

**Activation of spontaneously dividing T cell hybridomas induces interleukin-2 (IL-2) production, a cell cycle block, and programmed cell death. T cell hybridomas that express the T cell antigen receptor (TCR) ζ homodimer ($\zeta_2$), but not the TCR ζη heterodimer, were studied. The $\zeta\eta^-$ cells produced little or no inositol phosphates (IP) when stimulated with antigen. In most cases the hydrolysis of phosphoinositides was also impaired after stimulation with antibody to CD3, although one $\zeta\eta^-$ cell produced normal concentrations of IP. The $\zeta\eta^-$ cells slowed their growth and secreted IL-2 in response to both stimuli. However, the $\zeta\eta^-$ cells did not die after activation with antigen. Since activated thymocytes also undergo programmed cell death, these results may have important implications for the role of the ζη TCR in negative selection.**

WE HAVE RECENTLY FOUND THAT transfection of a $\zeta^-$ variant of the 2B4.11 antigen–specific T cell hybridoma with ζ cDNA restored cell surface TCR levels to normal, but did not reconstitute η expression (we were unable to detect any ζη with techniques that would have allowed us to detect levels that are as low as ~0.2% that of 2B4.11) (*1*). A series of subclones from two independent $\zeta\eta^-$ transfectants, 2A7 and 1.2, were analyzed for their responses to transmembrane activation. Because previously isolated $\zeta\eta^{low}$ cells had been found to generate IP poorly in response to antigen or a monoclonal antibody (MAb) to CD3-ε (anti-CD3), 2C11 (*2*), the production of IP in the $\zeta\eta^-$ cells was measured (Fig. 1). Antigen caused 2B4.11 cells to generate large amounts of IP; in contrast, all of the $\zeta\eta^-$ subclones produced low to undetectable quantities (Fig. 1A). IP production was observed when anti-CD3 was used to stimulate the cells (Fig. 1B). However, the maximal response was generally low, being only 5 to 30% of that of 2B4.11 cells. An exception to this was the subclone 1.2.2, in which the level of 2C11-stimulated IP approached that of 2B4.11. We could not find any unusual structural property of this subclone to explain its relatively normal IP production when stimulated this way. This same $\zeta\eta^-$ subclone yielded very little IP in response to antigen (Fig. 1A). This difference could not be attributed to a dose-response effect, since antigen failed to generate IP production even at very high concentrations (compare Fig. 1, C and D).

M. Merćep and J. D. Ashwell, Biological Response Modifiers Program, National Cancer Institute, National Institutes of Health, Bethesda, MD 20892.
A. M. Weissman, S. J. Frank, R. D. Klausner, Cell Biology and Metabolism Branch, National Institute of Child Health and Human Development, National Institutes of Health, Bethesda, MD 20892.

*Present address: Experimental Immunology Branch, National Cancer Institute, National Institutes of Health, Bethesda, MD 20892.

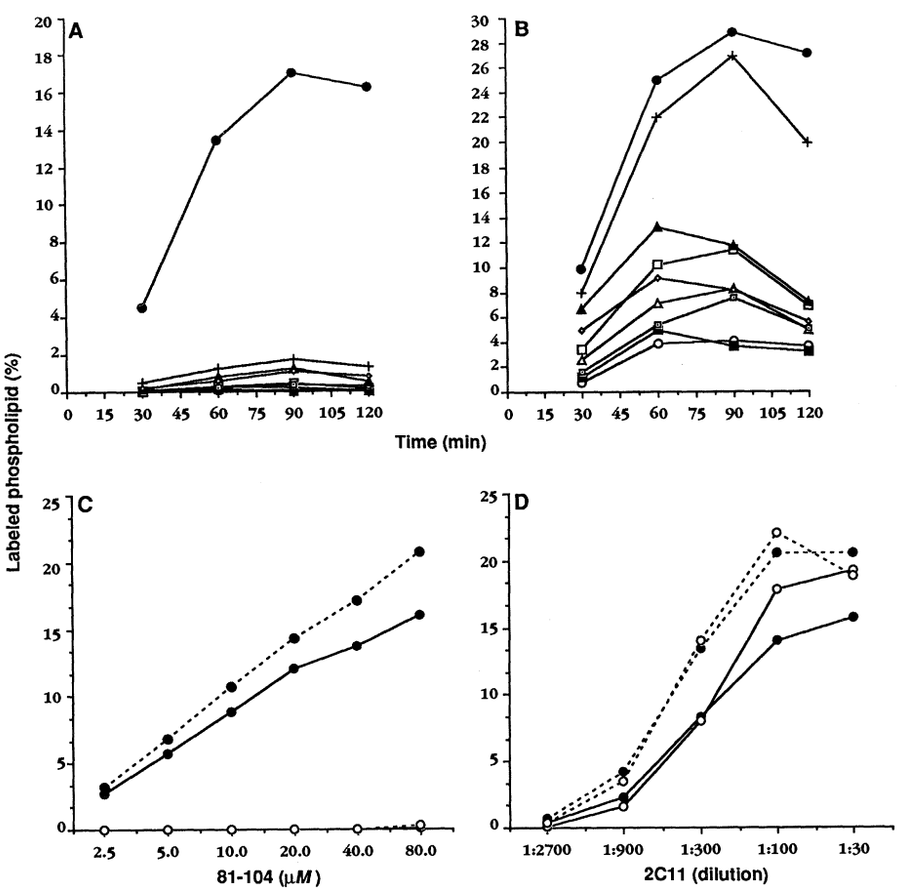


**Fig. 1.** IP production as a function of TCR ζη expression. The 2B4.11 T cell hybridoma or its $\zeta\eta^-$ variants were loaded with $^3$H-labeled *myo*-inositol. Labeled T cells ($1 \times 10^6$ per experimental point) were incubated with $10^6$ LK-35.2 cells [LK, class II–bearing B hybridoma cells (*10*)] plus (**A**) a fixed amount of pigeon cytochrome c amino acids fragment 81–104 (20 μ*M*), (**B**) 2C11 (1:30 dilution of culture supernatant), (**C**) the indicated concentrations of pigeon cytochrome c amino acids 81–104, or (**D**) the indicated concentrations of 2C11. At the indicated times the cells were lysed and the amount of water soluble–labeled IP was determined as described in (*11*). The data are expressed as the amount of radioactivity recovered from the IP fraction divided by the total amount of label incorporated by the cell (×100). The data in (A) and (B) are compiled from three independent experiments in which different $\zeta\eta^-$ cells were tested; 2B4.11 cells were included in each assay as a control for comparison; the data are displayed in one graph for simplicity. IP generation by 2B4.11 cells was similar in all experiments, with the maximal amount ranging from 14.4 to 17.0% in response to antigen. The 2A7 (protoplast fusion) and 1.2 (electroporation) cell lines were made by transfecting a ζ chain–negative 2B4.11 variant (*11*) with cDNA encoding the murine ζ chain (*1*). Subclones of 2A7 and 1.2 were obtained by a limiting dilution of 0.3 cells per well in flat-bottomed 96-well microtiter plates (no. 3596, Costar) in RPMI 1640 (Biofluids) supplemented with 7.5% heat-inactivated fetal calf serum, 4 m*M* glutamine, penicillin (100 U/ml), gentamicin (150 mg/ml), and $5 \times 10^{-5}$ *M* 2-mercaptoethanol (complete medium). The subclones 2A7.1, 2A7.7, 2A7.11, 2A7.33, 2A7.37, 1.2.2, 1.2.3, and 1.2.7 were chosen for further study because they stably expressed cell surface TCR levels that were comparable to that of 2B4.11. (A) and (B): ●, 2B4.11; □, 2A7.1; ○, 2A7.7; △, 2A7.11; ■, 2A7.33; ⊡, 2A7.37; +, 1.2.2; ▲, 1.2.3; and ◇ 1.2.7. (C) and (D): ●, 2B4.11; ○, 1.2.2; ——, 60 min; and ---, 90 min.

Stimulation with $AlF_4^-$, a direct activator of G protein–dependent phospholipase C activity (*3*), caused the generation of similar amounts of IP from 2B4.11 cells and each of the $\zeta\eta^-$ subclones. Therefore, these $\zeta\eta^-$ subclones differ from previously characterized $\zeta\eta^{low}$ cells in that although generally blunted, phosphoinositide (PI) hydrolysis could be initiated via the $\zeta_2$-containing TCR by cross-linking with anti-CD3. In concordance with the previous studies, however, PI hydrolysis initiated by occupancy of the TCR was dependent on the $\zeta\eta$ heterodimer.

Unlike the previously characterized $\zeta\eta^{low}$ cells (*2*), the $\zeta\eta^-$ transfectants produced IL-2 when stimulated with phorbol myristate acetate (PMA) plus ionomycin. Therefore, 2B4.11 and its variants were tested for their ability to secrete IL-2 in response to TCR-mediated signals. All of the T cell hybridomas produced IL-2 in response to antigen or anti-CD3 (Fig. 2). There was a considerable degree of variation in the maximal amount of IL-2 produced by each subclone, as well as some day-to-day variability in the dose-response curves. However, no correlation was found between the amount of IL-2 produced and the levels of $\zeta\eta$. Furthermore, the half-maximal responses of the clones were generally within a threefold range in individual experiments. In contrast to normal peripheral T cells, T cell hybridomas are growth inhibited soon after stimulation (*4*). The growth of 2B4.11 and all of the $\zeta\eta^-$ T cell clones was slowed equivalently after stimulation with antigen or anti-CD3 MAb. Therefore, the $\zeta_2$-TCR is capable of transducing all of the signals required for initiating IL-2 secretion and inhibition of growth. In addition, the finding that antigen stimulated two TCR-dependent biological responses in the $\zeta\eta^-$ cells proves that its failure to induce PI hydrolysis was not due to lack of recognition.

The activation-induced growth inhibition of T cell hybridomas is accompanied by cell lysis and genomic DNA fragmentation (*5*). Because the cell-cycle block and the cell death appear to be the result of different intracellular pathways, the ability of TCR-mediated signals to induce cell lysis was investigated (Fig. 3). In contrast to IL-2 production and incorporation of [$^3$H]thymidine, cell lysis in response to antigen stimulation was clearly different between $\zeta\eta^+$ and $\zeta\eta$-deficient subclones. The 2M.51 subclone, which expresses slightly more $\zeta\eta$ than 2B4.11 cells, lysed as well as, if not better than, 2B4.11. The 2M.143 subclone, containing about 20% less $\zeta\eta$ than 2B4.11, exhibited significant lysis in response to antigen, although at a higher antigen concentration and with less total specific $^{51}$Cr release. In contrast, the $\zeta\eta^-$ subclones manifested relatively little lysis. To determine how far this correlation could be extended, we tested other independently derived $\zeta\eta$-deficient 2B4.11 subclones for activation-induced death. The T$\alpha\beta$1.2 subclone contains ~60% less $\zeta\eta$, and the $\zeta\eta$-deficient EV.3 subclone 90 to 95% less $\zeta\eta$, than 2B4.11 (*2*); neither cell lysed when stimulated with antigen. Although causing some lysis in $\zeta\eta^-$ cells, anti-CD3–induced lysis was more efficient in $\zeta\eta^+$ cells (Fig. 2B). The correlation between $\zeta\eta$ loss and the phenotypes described above is not unique to the MA5.8 cell line, from which these transfectants were derived. We have also transfected a newly derived 2B4.11 $\zeta$ chain-loss variant with $\zeta$ cDNA. This cell also expresses no detectable $\zeta\eta$, and its phenotype with regard to antigen-driven PI hydrolysis (maximal hydrolysis of labeled phospholipid: 15% for 2B4.11 cells and 0.2% for the $\zeta\eta^-$ variant) and cell death (specific $^{51}$Cr release induced by 30 $\mu M$ antigen: 24% for 2B4.11 cells and 2% for the $\zeta\eta^-$ variant) was indistinguishable from the MA5.8-derived $\zeta\eta^-$ subclones. In contrast to MA5.8, this $\zeta\eta^-$ variant was not derived by chemical mutagenesis. These data indicate that there is a positive relation between $\zeta\eta$ expression and the death of T cell hybridomas activated with antigen, although it is not a linear one. This may indicate that there is a threshold

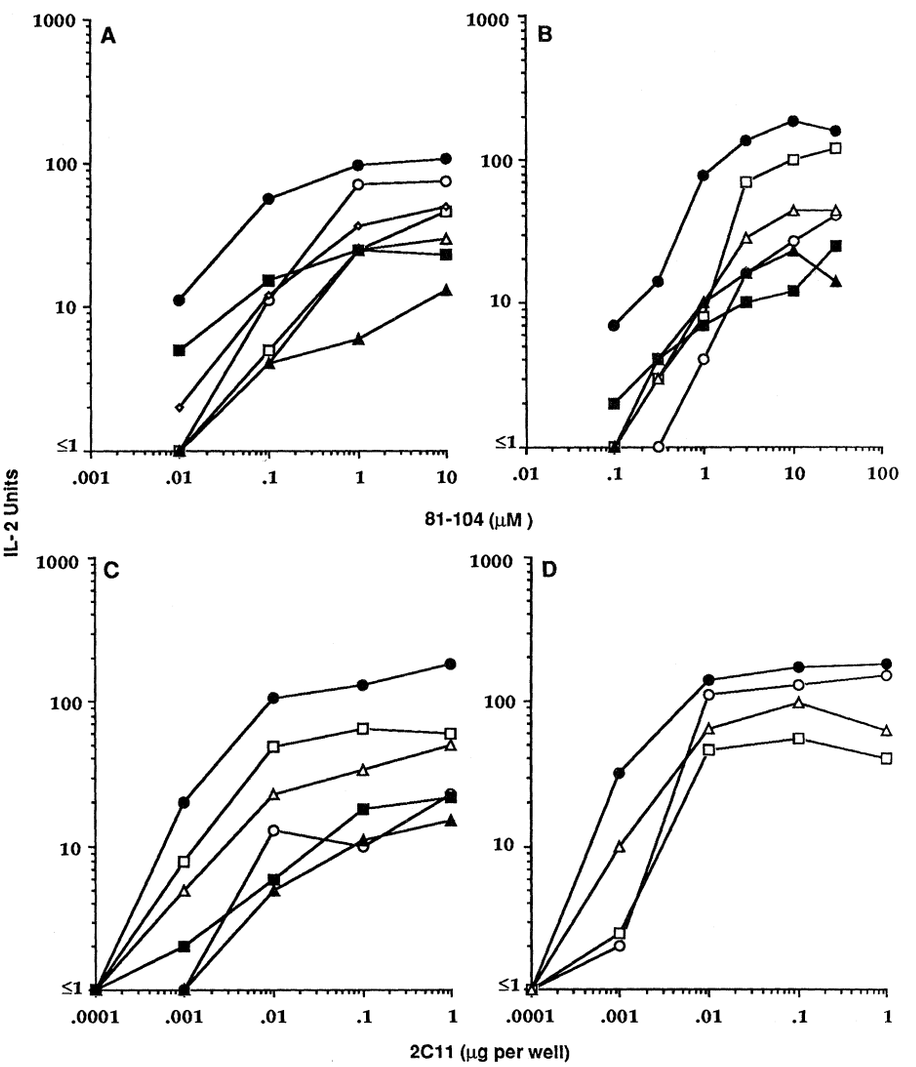


**Fig. 2.** IL-2 production in response to antigen or immobilized anti-CD3. Antigen stimulated T cell hybridomas ($2 \times 10^4$) were incubated with either $2 \times 10^4$ (**A**) or $10^4$ (**B**) irradiated (10,000 rads) LK cells in the presence of the indicated concentrations of pigeon cytochrome c amino acids 81–104. Anti-CD3 stimulation (**C** and **D**): T cell hybridomas ($2 \times 10^4$) were placed into microtiter wells that had been pre-incubated with the indicated concentrations of the purified 2C11 MAb. After an overnight culture, aliquots of supernatant were assayed for IL-2 content. Closed symbols represent 2B4.11 or its subclones that express $\zeta\eta$; open symbols represent derivatives of 2B4.11 that are $\zeta\eta^-$. Each graph represents an independent experiment. (A) ●, 2B4.11; ○, 2A7.1; □, 2A7.11; △, 2A7.33; ◇, 2A7.37; ■, 2M.51; and ▲, 2M.143. (B and D) ●, 2B4.11; ○, 1.2.2; □, 1.2.3; △, 1.2.7; ■, 2M.51; and ▲, 2M.143. (C) ●, 2B4.11; ○, 2A7.7; □, 2A7.33; △, 2A7.37; ■, 2M.51; and ▲, 2M.143.

diminished, or that the ratio of $\zeta\eta$ to $\zeta_2$ determines the efficiency of signaling for cell death.

The different $\zeta\eta^-$ cells used to characterize the death of T cell hybridomas after activation were derived over several years and by a variety of methods. The $\zeta\eta^+$ subclones 2M.51 and 2M.143, for example, were derived from the same 2C11-inoculated animal as EV.3. The TCR β chain–negative 21.2.2 cell (the parent of the Tαβ1.2 cell) was derived by repetitive subcloning. The $\zeta^-$ MA5.8 cell was isolated after mutagenesis and incubation in the presence of antigen; its loss of cell surface–TCR expression is sufficient to account for its growth under these conditions. Therefore, we think it unlikely that a second mutation, independent of $\zeta\eta$ expression and common to all of these cells, could explain their lack of lysis when exposed to even supraoptimal doses of antigen. However, to explicitly test whether these cells could be induced to undergo programmed cell death by stimuli that bypass the TCR, we measured DNA fragmentation in response to dexamethasone (Fig. 4). Dexamethasone caused the 2B4.11 wild-type cell and two $\zeta\eta$-deficient variants to manifest the DNA fragmentation characteristic of programmed cell death. As with $^{51}Cr$ release, only 2B4.11 cells manifested DNA fragmentation when stimulated with antigen. These results suggest that the coupling of the TCR to programmed cell death is specifically affected in the $\zeta\eta$ variant cells.

These studies demonstrate a difference between the response of $\zeta\eta^-$ cells to antigen and to anti-CD3. A similar phenomenon has been previously seen with 2B4.11 cells (*6*): the protein kinase C–mediated phosphorylation of CD3-γ after activation with anti-CD3, anti–Thy-1, or antigen was inhibited at identical concentrations of cyclic adenosine monophosphate (cAMP), as was the antigen-stimulated tyrosine phosphorylation of ζ. In contrast, cAMP did not block the tyrosine phosphorylation of ζ in response to anti-CD3 or anti–Thy-1. In $\zeta^-$ MA5.8 cells, stimulation with immobilized or cross-linked anti-CD3 was able to induce IL-2 secretion (7), whereas stimulation with antigen generated very little IL-2. With thymocytes, a dichotomy has been observed between anti-αβ and anti-CD3–induced $Ca^{2+}$ mobilization (*8*). It is likely that receptor occupancy is fundamentally different from physical cross-linking by high-affinity immobilized or cross-linked antibody. Furthermore, because of different associations between the TCR components, cross-linking of αβ may have different biological effects than cross linking of CD3. We have not yet tested the effects of αβ cross-linking on the $\zeta\eta^-$ subclones.

Activation-induced growth inhibition comprises an early (within minutes) $G_1/S$ cell cycle block that is resistant to cyclosporine A (CsA) and the later (4 to 6 hour) occurrence of cell death and DNA fragmentation that is prevented by CsA (*5*). Bearing in mind that T cell hybridomas are the product of a fusion between antigen-specific peripheral T cells and an AKR-derived thymoma, the lysis of transformed T cells like 2B4.11 may provide a useful model for the physiological response of developing T cells that are eliminated when they encounter self antigens in the thymus (that is, negative selection) (*4, 5*). This possibility is made even more attractive by the observation that clonal deletion in the thymus is prevented by CsA (*9*). Furthermore, it has recently been found that activation of both T cell hybridomas and thymocytes results in DNA fragmentation, a process that is prevented by CsA (*5*). If 2B4.11 represents a cellular phenotype similar to that of thymocytes

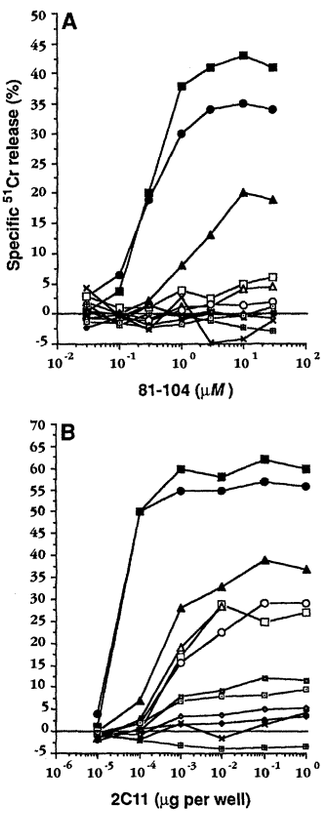


**Fig. 3.** Cell lysis after stimulation. T cell hybridomas were loaded with $^{51}Cr$ and cultured at a density of $3 \times 10^4$ per well with (**A**) varying concentrations of pigeon cytochrome c fragment 81–104 plus $2 \times 10^4$ irradiated LK cells, or (**B**) anti-CD3–coated wells, as described (*12*). After 12 hours the supernatant was harvested from each well and specific $^{51}Cr$ release was calculated with the formula:

$$\text{Percent specific } ^{51}\text{Cr release} = \frac{\text{Experimental release} - \text{Spontaneous release}}{\text{Maximal release} - \text{Spontaneous release}} \times 100$$

The standard error of the mean was always ≤5% for each determination. In addition to the 2A7 and 1.2 $\zeta\eta^-$ cell lines (described in legend to Fig. 1), Tαβ1.2 and EV.3 are $\zeta\eta$-deficient subclones of 2B4.11. The Tαβ1.2 cell line was created by transfecting a β chain–negative 2B4.11 mutant with the original 2B4 α and β chains (*13*) and expresses ~60% less $\zeta\eta$ than 2B4.11 cells (*2*). The clone EV.3 was isolated from a mouse that had been inoculated with viable 2B4.11 cells and then treated with intraperitoneal injections of an anti-CD3 MAb; it expresses ~5% as much $\zeta\eta$ as 2B4.11 cells (*2*). ●, 2B4.11; ■, 2M.51; ▲, 2M.143; ⊞, Tαβ1.2; □, 1.2.2; △, 1.2.3; ○, 1.2.7; ◇, 2A7.1; ◆, 2A7.7; ▣, 2A7.33; ⊡, 2A7.37; and ×, EV.3.

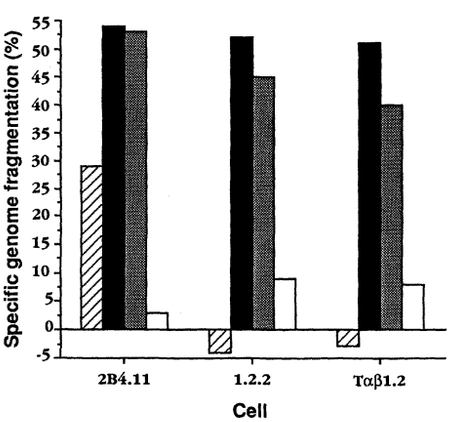


**Fig. 4.** Genome fragmentation in response to antigen or dexamethasone. Measurement of DNA autolysis was modified from the procedure of Duke *et al.* (*14*). Briefly, the indicated T cell hybridomas ($4 \times 10^6$/ml) were labeled with 100 μCi of [$^3$H]thymidine during a 2-hour culture. After a thorough washing, $2 \times 10^5$ cells were cultured in 5-ml tubes with $10^5$ LK cells (10,000 rad) plus 20 μ*M* pigeon cytochrome c amino acids 81–104 or the indicated concentrations of dexamethasone. After 16 hours, the cells were centrifuged and the supernatants collected. The cells were then lysed in a buffer consisting of 10 m*M* tris, 1 m*M* EDTA, and 0.2% Triton X-100, *p*H 7.5 (lysis buffer). After 30 min on ice, the lysates were centrifuged to separate fragmented DNA from intact chromatin. All fractions were analyzed for $^3H$ content by scintillation counting, and the percent specific DNA fragmentation was calculated according to the formula:

$$\text{Percent specific DNA fragmentation} = \frac{\text{cpm}_{\text{sup}} + \text{cpm}_{\text{lysate}} - \text{cpm}_{\text{spontaneous}}}{\text{cpm}_{\text{total}} - \text{cpm}_{\text{spontaneous}}} \times 100$$

where $\text{cpm}_{\text{sup}}$ is the cpm in the incubation medium, $\text{cpm}_{\text{lysate}}$ is cpm in the supernatant after the nuclei have been removed by centrifugation and $\text{cpm}_{\text{total}}$ is cpm in all three fractions (supernatant, lysate, and pellet). The $\text{cpm}_{\text{spontaneous}}$ was determined by incubating labeled cells in medium in the absence of any stimulus. Hatched bars, 81–104 (20 μ*M*); solid bars, dexamethasone ($10^{-6}$*M*); stippled bars, dexamethasone ($10^{-8}$*M*); and clear bars, dexamethasone ($10^{-10}$*M*).

susceptible to TCR-initiated cell death, the implication is that there may be a specific role for ζη-containing TCRs in the deletion of anti-self thymic T cells. In such a model, the biological responses of T cells at different stages of development might depend on the composition of their TCRs, or there may be stage-specific variation in the cellular response to ζη-TCR occupancy because of altered receptor coupling or cellular receptivity to these signals. It may be possible to test this speculation by quantitating $\zeta_2$ and ζη expression in developing thymocytes.


REFERENCES AND NOTES

1. A. M. Weissman *et al.*, *EMBO J.*, in press.
2. M. Mercep *et al.*, *Science* **242**, 571 (1988).
3. P. C. Sternweis and A. G. Gilman, *Proc. Natl. Acad. Sci. U.S.A.* **79**, 4888 (1982); P. F. Blackmore, S. B. Bocckino, L. E. Waynick, J. H . Exton, *J. Biol. Chem.* **260**, 14477 (1985); J. J. O'Shea *et al.*, *J. Immunol.* **139**, 3463 (1987).
4. J. D. Ashwell, R. E. Cunningham, P. D. Noguchi, D. Hernandez, *J. Exp. Med.* **165**, 173 (1987).
5. M. Mercep, P. D. Noguchi, J. D. Ashwell, *J. Immunol.* **142**, 4085 (1989); Y. Shi, B. M. Sahai, D. R. Green, *Nature* **339**, 625 (1989); D. Ucker, J. D. Ashwell, G. Nickas, *J. Immunol.*, in press.
6. R. D. Klausner *et al.*, *J. Biol. Chem.* **262**, 12654 (1987).
7. J. J. Sussman *et al.*, *Cell* **52**, 85 (1988).
8. T. H. Finkel, P. Marrack, J. W. Kappler, R. T. Kubo, J. C. Cambier, *J. Immunol.* **142**, 3006 (1989).
9. M. K. Jenkins, R. H. Schwartz, D. M. Pardoll, *Science* **241**, 1655 (1988); E.-K. Gao *et al.*, *Nature* **336**, 176 (1988).
10. J. Kappler, J. White, D. Wegmann, E. Mustain, P. Marrack, *Proc. Natl. Acad. Sci. U.S.A.* **79**, 3604 (1982).
11. J. J. Sussman *et al.*, *Nature* **334**, 625 (1988).
12. M. Mercep, J. A. Bluestone, P. D. Noguchi, J. D. Ashwell, *J. Immunol.* **140**, 324 (1988).
13. J. J. Sussman, T. Saito, E. M. Shevach, R. N. German, J. D. Ashwell, *ibid.*, p. 2520.
14. R. C. Duke, R. Chervenak, J. J. Cohen, *Proc. Natl. Acad. Sci. U.S.A.* **80**, 6361 (1983).


12 July 1989; accepted 18 October 1989

# Second Cytotoxic Pathway of Diphtheria Toxin Suggested by Nuclease Activity

MICHAEL P. CHANG,* RAE LYNN BALDWIN, CAN BRUCE, BERNADINE J. WISNIESKI†

**Diphtheria toxin (DTx) provokes extensive internucleosomal degradation of DNA before cell lysis. The possibility that DNA cleavage stems from direct chromosomal attack by intracellular toxin molecules was tested by in vitro assays for a DTx-associated nuclease activity. DTx incubated with DNA in solution or in a DNA-gel assay showed $Ca^{2+}$- and $Mg^{2+}$-stimulated nuclease activity. This activity proved susceptible to inhibition by specific antitoxin and migrated with fragment A of the toxin. Assays in which supercoiled double-stranded DNA was used revealed rapid endonucleolytic attack. Discovery of a DTx-associated nuclease activity lends support to the model that DTx-induced cell lysis is not a simple consequence of protein synthesis inhibition.**

THE KILLING MECHANISM OF DIPHtheria toxin (DTx) is widely accepted as being exclusively linked to its ability to inhibit protein synthesis in eukaryotic cells via adenosine diphosphate (ADP)–ribosylation of elongation factor 2 (*1*). The ADP-ribosyl (ADPr) transferase activity is ascribed to the A domain of cleaved, reduced toxin; the B or receptor-binding domain has no known enzymatic activity. We had identified two relatively early markers for DTx-triggered cytolysis, the appearance of widespread membrane blebbing and extensive prelytic internucleosomal DNA cleavage, and showed that these properties are not associated with protein synthesis inhibition per se but with DTx treatment (*2*). On the basis of these observations, we proposed that DTx might activate an endogenous nuclease-dependent suicide pathway akin to cytotoxic models established for glucocorticoid hormones (*3*), cytotoxic effector cells (*4*), ionizing radiation (*5*), and the compound 2,3,7,8-tetrachlorodibenzo-*p*-dioxin (*6*). We have now investigated the possibility that DTx might itself catalyze target cell DNA degradation rather than serve to activate an endogenous nuclease.

Human U937 target cells begin to show evidence of DNA fragmentation about 5 hours after exposure to DTx (Fig. 1A, lane 4). The characteristic ladder pattern of DNA breakdown is indicative of internucleosomal DNA degradation (*7*), which precedes DTx-triggered cytolysis by 2 to 3 hours (*2*). The early triggering of DNA fragmentation is not observed with cycloheximide (Fig. 1A, lane 5) or sodium azide plus 2-deoxyglucose (Fig. 1A, lane 6), even though these agents lead to rapid and prolonged inhibition of translation activity in U937 cells (*2*). Addition of DTx to DNA extracted from untreated cells also provoked extensive cleavage (Fig. 1A, lane 1). The degradation profile suggests progressive destruction of DNA into small fragments. Sham-treated DNA displayed no loss of integrity (Fig. 1A, lane 2). Since studies of cell suicide processes revealed that endogenous nuclease activation requires $Ca^{2+}$ and $Mg^{2+}$, the effect of adding these cations was tested. The presence of both cations caused a very marked enhancement of toxin-associated deoxyribonuclease (DNase) activity (Fig. 1B). Detection of nuclease activity in the presence of 1 m*M* EDTA (Fig. 1A, lane 1) required extended incubation.

DTx incubated with lambda phage DNA provoked marked DNA degradation (Fig. 1C, lane 3), whereas buffer fractions (containing no DTx) from the same column elicited no DNA degradation (Fig. 1C, lane 7). Moreover, addition of DTx-specific antibody completely blocked the nuclease activity of the DTx (Fig. 1C, lane 4). The antibody also inhibited purified monomer preparations of DTx. Nonspecific antibodies had no effect on the DTx-associated nuclease activity (Fig. 1C, lane 6).

To discount the presence of nuclease contaminants that might be sensitive to antitoxin inhibition, we subjected samples of "intact" DTx (*8*) and Arg-C–cleaved DTx (*9*) to electrophoresis under reducing conditions on SDS-polyacrylamide gels that contained embedded DNA (Fig. 2). After being washed to remove SDS, the gels were incubated for 24 hours in 40 m*M* tris buffer (*p*H 7.6) with $MgCl_2$ and $NaN_3$. The absence of ethidium bromide staining was used to detect nuclease activity. As expected (*10*), pancreatic DNase I showed no activity with $MgCl_2$ (Fig. 2, lane c). However, nuclease activity was observed in the cleaved toxin sample at a position corresponding to DTx fragment A (Fig. 2, lane b at 24 hours). After a second 24-hour incubation in buffer containing $CaCl_2$ plus $MgCl_2$, DNase I gave the predicted positive response (Fig. 2, lane d), and an activity corresponding to the A domain of "intact" DTx appeared (Fig. 2, lane a at 48 hours). At this time, the size of the DNA-negative area associated with the A domain of the nicked DTx increased significantly (Fig. 2, lane b at 48 hours). Indeed, the observation that the nuclease

Department of Microbiology and The Molecular Biology Institute, University of California, Los Angeles, CA 90024.

*Present address: Department of Pharmacy, University of California, San Francisco, CA 94143.
†To whom correspondence should be addressed.